University of Reading

CO2 emissions from karst cascade hydropower reservoirs: mechanisms and reservoir effect

Article

Published Version

Creative Commons: Attribution 4.0 (CC-BY)

Open Access

Wang, W., Li, S.-L., Zhong, J., Wang, L., Yang, H. ORCID: https://orcid.org/0000-0001-9940-8273, Xiao, H. and Liu, C.-Q. (2021) CO2 emissions from karst cascade hydropower reservoirs: mechanisms and reservoir effect. Environmental Research Letters, 16 (4). 044013. ISSN 1748-9326 doi: https://doi.org/10.1088/1748-9326/abe962 Available at https://centaur.reading.ac.uk/96904/

It is advisable to refer to the publisher's version if you intend to cite from the work. See Guidance on citing.

To link to this article DOI: http://dx.doi.org/10.1088/1748-9326/abe962

Publisher: Institute of Physics

All outputs in CentAUR are protected by Intellectual Property Rights law, including copyright law. Copyright and IPR is retained by the creators or other copyright holders. Terms and conditions for use of this material are defined in the End User Agreement.

www.reading.ac.uk/centaur

University of Reading

CentAUR

Central Archive at the University of Reading

Reading's research outputs online

ENVIRONMENTAL RESEARCH
LETTERS

LETTER • OPEN ACCESS

CO_2 emissions from karst cascade hydropower reservoirs: mechanisms and reservoir effect

To cite this article: Wanfa Wang *et al* 2021 *Environ. Res. Lett.* **16** 044013

View the article online for updates and enhancements.

This content was downloaded from IP address 134.225.255.38 on 16/03/2021 at 15:03

ENVIRONMENTAL RESEARCH
LETTERS

LETTER

CO_2 emissions from karst cascade hydropower reservoirs: mechanisms and reservoir effect

Wanfa Wang[1], **Si-Liang Li**[1,2,*], **Jun Zhong**[1], **Lichun Wang**[1], **Hong Yang**[3], **Huayun Xiao**[1] **and Cong-Qiang Liu**[1]

[1] Institute of Surface-Earth System Science, School of Earth System Science, Tianjin University, Tianjin 300072, People's Republic of China
[2] State Key laboratory of Hydraulic Engineering Simulation and Safety, Tianjin University, Tianjin 300072, People's Republic of China
[3] Department of Geography and Environmental Science, University of Reading, Whiteknights, Reading RG6 6AB, United Kingdom
[*] Author to whom any correspondence should be addressed.

E-mail: siliang.li@tju.edu.cn

Keywords: CO_2 emissions, cascade reservoirs, hydraulic retention time, $\delta^{13}C_{CO2}$, reservoir effect index

Supplementary material for this article is available online

OPEN ACCESS

RECEIVED
14 September 2020

REVISED
22 February 2021

ACCEPTED FOR PUBLICATION
24 February 2021

PUBLISHED
12 March 2021

Original content from this work may be used under the terms of the Creative Commons Attribution 4.0 licence.

Any further distribution of this work must maintain attribution to the author(s) and the title of the work, journal citation and DOI.

Abstract

Carbon dioxide (CO_2) emissions from aquatic surface to the atmosphere has been recognized as a significant factor contributing to the global carbon budget and environmental change. The influence of river damming on the CO_2 emissions from reservoirs remains poorly constrained. This is hypothetically due to the change of hydraulic retention time (HRT) and thermal stratification intensity of reservoirs (related to the normal water level, NWL). To test this hypothesis, we quantified CO_2 fluxes and related parameters in eight karst reservoirs on the Wujiang River, Southwest China. Our results showed that there was a significant difference in the values of pCO_2 (mean = 3205.7 μatm, SD = 2183.4 μatm) and $\delta^{13}C_{CO2}$ (mean = −18.9‰, SD = 1.6‰) in the cascade reservoirs, suggesting that multiple processes regulate CO_2 production. Moreover, the calculated CO_2 fluxes showed obvious spatiotemporal variations, ranging from −9.0 to 2269.3 mmol m^{-2} d^{-1}, with an average of 260.1 mmol m^{-2} d^{-1}. Interestingly, the CO_2 flux and $\delta^{13}C_{CO2}$ from reservoirs of this study and other reservoirs around the world had an exponential function with the reservoir effect index (R_i, HRT/NWL), suggesting the viability of our hypothesis on reservoir CO_2 emission. This empirical function will help to estimate CO_2 emissions from global reservoirs and provide theoretical support for reservoir regulation to mitigate carbon emission.

1. Introduction

Carbon dioxide (CO_2) is one of the dominant greenhouse gases (GHGs), contributing 65% to global warming effects that has led to many environmental problems (Smith *et al* 2013), such as glacier melting, sea-level rise (Deemer *et al* 2016). Therefore, it is critical to fully understand the global carbon cycle, especially regarding CO_2 emissions from inland waters that was regarded as an important game player (Tranvik *et al* 2009, Raymond *et al* 2013, Räsänen *et al* 2018, Li *et al* 2018b, Maavara *et al* 2020). For example, Cole *et al* (2007) have estimated that 0.75 Pg C y^{-1} in terms of CO_2 flux outgassed from inland waters, while Raymond *et al* (2013) proposed that CO_2 outgassing rate can be up to 2.1 Pg C y^{-1}. Aside from natural processes, anthropogenic activities further exacerbate global environmental change by establishing numerous dams on rivers at the global scale where GHGs significantly emerge from the dam-regulated reservoir surface and degas from the released water (St. Louis *et al* 2000, Abril *et al* 2005, Guérin *et al* 2006, Barros *et al* 2011, Deemer *et al* 2016, Li 2018c, Liang *et al* 2019, Chen *et al* 2021). The dams are favorable since hydropower station has been regarded as a 'green' energy source for providing an inexhaustible supply of electrical power (ICOLD). Till now, more than 67% of the world's rivers have been dammed, especially in densely populated and energy-deficient areas (Grill *et al* 2019).

It is well known that cascade reservoirs have aggravated the fragmentation of rives, leading to the

© 2021 The Author(s). Published by IOP Publishing Ltd

appreciable changes in the carbon biogeochemical behavior (Grill *et al* 2015, Gibson *et al* 2017, Li *et al* 2018b, Wang *et al* 2020a, Yi *et al* 2021). Many researchers have studied the CO_2 emissions from individual reservoirs (Huttunen *et al* 2003, Guérin *et al* 2006, Pu *et al* 2020), but only a few scholars researched CO_2 production and emission mechanism of cascade reservoirs with different hydrodynamic conditions, altitudes, and artificial regulation (Li *et al* 2015, 2018a, Shi *et al* 2017). This is particularly important for cascade reservoirs located in the karst region, since carbonate weathering of karst rivers has been recognized as an important carbon sink, which markedly influences the global carbon cycling (Ford and Williams 2007). Carbonate weathering would cause the proportion of bicarbonate (HCO_3^-) to be more than 80% of the total anions in waters (Gaillardet *et al* 1999, Meybeck 2003), resulting in higher dissolved inorganic carbon (DIC) concentration in karst rivers (Beaulieu *et al* 2012, Goudie and Viles 2012). Moreover, the mineralization of organic matter (OM) is the dominant source of CO_2 in the reservoirs (Barros *et al* 2011, Shi *et al* 2017) and would lead to lower pH in the hypolimnion and released water, accelerating the dissolution of carbonate rocks and causing higher pCO_2 (Guérin *et al* 2006, Pu *et al* 2019, Wang *et al* 2020a). Thus, karst reservoirs may enhance carbon cycle and result in more CO_2 emission to atmosphere (Huttunen *et al* 2003, Butman and Raymond 2011).

Although the effect of single reservoirs on the carbon cycle has been studied, little is known about the river cascade damming with the distinct characteristics of different hydraulic retention time (HRT) by anthropogenic regulation (Wang *et al* 2015, Liang *et al* 2019). Moreover, different altitudes with the varying atmospheric temperature can affect the thermal stratification in the reservoirs and thus affect carbon transport and transformation (Barros *et al* 2011, Wang *et al* 2020a). To address the unresolved question on the effect of cascade reservoirs on carbon cycle regarding CO_2 emission, we hypothesized that CO_2 emission from cascade reservoirs is controlled by both of normal water level (NWL, a metric to represent the atmospheric temperature's effect) and HRT. To test this hypothesis, we calculated pCO_2, CO_2 fluxes and other relevant properties in eight reservoirs with different HRT and NWL on the Wujiang River, which located at the central karst area in Southwest China. Specifically, the CO_2 fluxes, water chemical parameters, stable carbon isotope, and environmental parameters were measured and quantified. By compiling exhaustive previous studies focusing on CO_2 emissions from the cascade reservoirs, our study demonstrate our hypothesis is viable. Importantly, the established predictive function between CO_2 fluxes and influencing factors (HRT and NWL) in this study allows to estimate the contribution of CO_2 emissions from reservoirs to global carbon budget.

2. Materials and methods

2.1. Study area

The Wujiang River is located in Southwest China, one of the largest karst region in the world (Ford and Williams 2007). It is also the largest tributary in the upper reaches and south bank of the Yangtze River with a subtropical monsoon humid climate (figure 1). The river has a total length of 1037 km, an area of 8.79×10^4 km^2, and an elevation difference of 2124 m, with the consequence of obvious spatiotemporal heterogeneity of air temperature (Wang *et al* 2020a). The climate is typical, rain and heat synchronization with rich rainfall (the average annual rainfall up to 1100 mm) and high air temperature (average annual temperature of 13 °C–18 °C), and more than 80% of the precipitation occurs in the warm season (April to September) (Wang *et al* 2020a). Due to the abundant hydropower resources (up to 1042.59×10^4 kw), more than 1000 dams have been built on Wujiang River, and it has been one of the ten hydropower bases in China (EBHHC 2007, Gzpwrd 2017).

In this study, we studied seven reservoirs along the mainstream including the reservoirs of Hongjiadu (HJD), Dongfeng (DF), Suofengying (SFY), Wujiangdu (WJD), Silin (SL), Pengshui (PS), and Yinpan (YP). Besides, Hongfeng (HF) reservoir in the main tributary (Maotiao River) was also investigated for a better comparison (figure 1). All the eight reservoirs have different serving roles and characteristics due to their physical geography, meteorology, and hydrologic feature. Specifically, HJD and HF reservoirs are responsible for regulating, shipping, storing industrial water, supply drinking water and irrigation in the upstream; DF, WJD and SL reservoirs are responsible for regulating and generating electricity, while SFY, PS, and YP reservoirs are mainly used for providing electricity. Thus, the Wujiang cascade reservoir system is an ideal place to study the cascade damming effect on CO_2 emissions in karst rivers, because of the various natural factors and anthropogenic regulations. The detailed information of the eight reservoirs are listed in table 1.

2.2. Field sampling and analysis

Four field surveys were conducted at 40 sites (figure 1) in January (Winter), April (Spring), July (Summer), and October (Autumn) 2017 for collecting the inflowing (mainstream and tributaries), lentic profiles, and released water of each reservoir (figure 1). The water samples of inflowing, reservoir surface and released water were collected at the water depth of 0.5 m. Water samples along vertical profiles were collected at different depths in different reservoirs and seasons. Specifically, the stratified sampling was conducted at the depth of 0.5, 5, 15, 30, 45, and 60 m in HJD (W2-W5), DF (W8-W9), SFY (W11) and WJD (W13-W16). The water samples were also collected

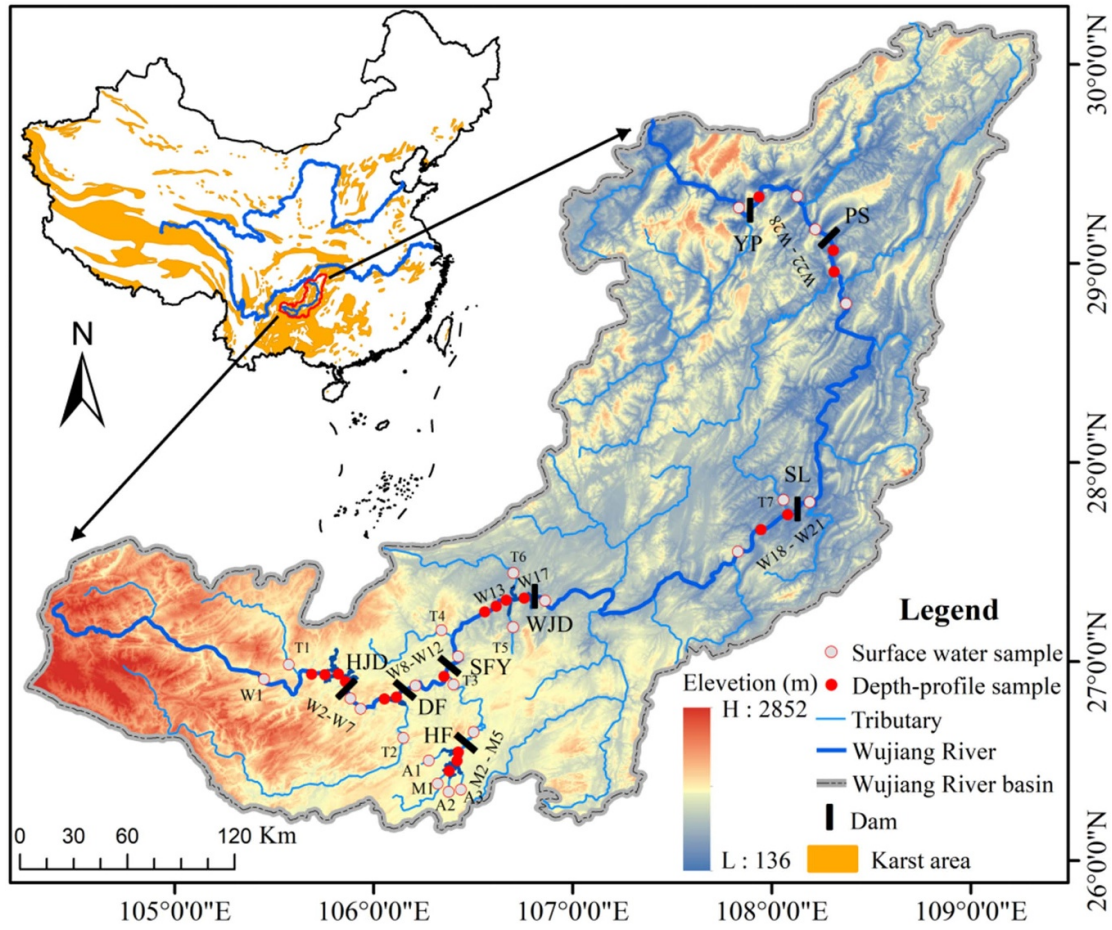

Figure 1. Location of cascade dams and sampling sites in the Wujiang River. Among the sampling sites, the capital letters 'W' and 'T' indicate sites located at the Wujiang River mainstream and its tributaries, while 'M' and 'A' indicate sites at the mainstream and the tributaries of the Maotiao River.

at the depths of 0.5, 10, 20, 30, and 60 m in SL (W19-W20) and PS (W23-W24), at the depth of 0.5, 5, 10, 20, 30, and 40 m in YP (W27) and at the depth of 0.5, 5, 10, 15, and 25 m in HF (M2-M4), respectively. We measured the physical and chemical properties of collected samples *in situ* using a multiparameter profiler (model: YSI EXO1), including water temperature (T_W), pH, dissolved oxygen (DO), oxygen saturation (DO (%)), and chlorophyll (Chl). The detail information about sampling and analysis for DIC, calcium ion (Ca^{2+}), partial pressure of CO_2 (pCO_2), and carbon isotope composition of DIC ($\delta^{13}C_{DIC}$) were shown in text S1 (supplementary materials) (available online at stacks.iop.org/ERL/16/044013/mmedia).

2.3. Estimation of CO_2 fluxes

The CO_2 fluxes (F_{CO2}) across the water-atmosphere interface in the cascade reservoirs were estimated based on a theoretical diffusion model proposed by Cole and Caraco (1998), Teodoru *et al* (2009), and Butman and Raymond (2011).

$$F_{CO2} = K_T \times K_H \times [pCO_2\,(\text{water}) - pCO_2\,(\text{air})] \quad (1)$$

$$K_H = 10^{-\left(1.11 + 0.016 - 0.00007 \times T^2\right)} \quad (2)$$

where F_{CO2} is the CO_2 flux from water to air unit in (mmol m^{-2} $d^{-1)}$, K_T is the exchange velocity of gas CO_2 (m d^{-1}), K_H is Henry's constant corrected for temperature T (°C) expressed in (mmol m^{-3} μatm^{-1}) (Harned and Davis 1943); $pCO_{2(water)}$ (μatm) is partial pressure CO_2 in the water (Clark and Fritz 1997). $pCO_{2(air)}$ is the partial pressure of CO_2 in the air (~400 μatm, based on www.esrl.noaa.gov/gmd/ccgg/trends/full.html).

The exchange velocity of CO_2 was determined by wind speed, current velocity, water temperature, and other factors (Wanninkhof 1992). K_T is the gas-exchange coefficient expressed in (cm h^{-1}) and it was calculated from the following equation from Jähne *et al* (1987).

$$K_T = K_{600} \times (S_c/600)^{-n} \quad (3)$$

$$K600 = 2.07 + 0.215U_{10}^{1.7} \quad (4)$$

$$S_c = 1911.1 - 118.11T + 3.4527T^2 - 0.04132T^3 \quad (5)$$

where K_{600} was calculated according to the equation from Cole and Caraco (1998). U_{10} (m s^{-1}) is the

Table 1. The basic characteristics of the studied reservoirs on the Wujiang River, Southwest China.

Reservoirs	Altitude (m)	Average air temperature (°C)	Catchment area (km^2)	Surface area (km^2)	Normal/dead water level (m)	Discharge (10^8 m^3 y^{-1})	Installed capacity (10 kw)	Storage coefficient[a] (%)	HRT[b] (d)	Year of construction	Type of regulation	Drainage basin
HJD	1093	15.2	9900	80.5	1140/1076	48.9	600	68.8	368	2001	Multi-year	Mainstream
DF	965	17.4	18 161	19.1	970/936	108.8	695	4.5	29	1994	Seasonal	Mainstream
SFY	850	17.4	21 862	5.7	835/813	134.7	600	0.6	4	2002	Daily	Mainstream
WJD	760	17.2	27 790	47.8	760/720	158.3	1250	8.5	49	1979	Seasonal	Mainstream
SL	457	20.3	48 558	38.4	440/431	266.2	1050	1.2	22	2006	Monthly	Mainstream
PS	336	20.6	69 000	15.3	293/278	410.0	1750	1.3	10	2003	Monthly	Mainstream
YP	285	20.2	74 910	11.4	215/211.5	438.4	600	0.1	3	2007	Daily	Mainstream
HF	1230	14.9	1596	57.2	1240/1227.5	9.2	20	48.2	302	1958	Multi-year	Tributary

[a] The storage coefficient (%) (β, the ratio of the mean reservoir regulation storage to the discharge) can represent the daily ($\beta < 1\%$), monthly ($1\% < \beta \leqslant 3\%$), seasonal ($3\% < \beta \leqslant 10\%$), yearly ($10\% < \beta \leqslant 30\%$) and multi-year ($30\% < \beta$) regulated reservoirs (Wang *et al* 2020a).

[b] HRT is hydraulic retention time.

frictionless wind speed at a height of 10 m above the water surface, and $n = 1/2$ or 2/3 for wind speeds exceeding 3.7 m s^{-1} or below 3.7 m s^{-1}, respectively (Guérin *et al* 2006). S_c is the Schmidt number for CO_2 in freshwater and it varies with temperature (Wanninkhof 1992). Considering the difficulty to carry out long-term monitoring on all sampling points and also data quality and representative, we collected the monthly average wind speed from meteorological stations (www.cma.gov.cn/) around the sampling points for the value of U_{10}.

Notably, in the warm season, when the low flow speed was <0.5 m s^{-1} in the reservoirs (HF, HJD, DF, WJD, and SL) with long HRT, the K_{600} was calculated using the equation (4). However, K_{600} can be affected by various factors such as wind speed, current, and turbidity (Guérin *et al* 2006, Raymond *et al* 2012). Due to the high flow speeds in the tributary, inflowing, released water, and short HRT in the run-of-river type reservoirs, the equation (4) may not appropriate for estimating K_{600}. Alternatively, we estimated K_{600} following Butman and Raymond (2011) and Raymond *et al* (2012):

$$K_{600} = 2.03 + S \times V \times 2841.6 \quad (6)$$

where S is the slope (‰) and V is river flow velocity (m s^{-1}). The detail information about the calculation of K_{600} at the sampling point with high flow speed has shown in the text S2.

Upon the estimated CO_2 flux as mentioned above, the CO_2 emissions (ton CO_2-C y^{-1}) from the reservoirs was calculated as the product of the average emission flux and the typical reservoir surface area, which was calculated based on the NWL of the reservoirs (Liang *et al* 2019).

2.4. Comprehensive analysis of chemical components

The water temperature dependence of the fractionation for ^{13}C between the DIC and CO_2 (aq) was calculated according to the following equation by Mook *et al* (1974) and Rau *et al* (1996).

$$\delta^{13}C_{CO2}(\%) = \delta^{13}C_{DIC} + 23.644 - 9701.5/(T + 273.15) \quad (7)$$

where T is the water temperature expressed in (°C) and the $\delta^{13}C$ value of DIC is approximately equal to that of HCO_3^- (Goudie and Viles 2012, Wang *et al* 2020a).

To reveal the major influencing factors and processes related to CO_2 emissions in cascade reservoirs, we calculated the changing degree of $\delta^{13}C_{CO2}$ (‰) and pCO_2 considering water going through reservoirs as follows (Wang *et al* 2020a):

$$\Delta\left[\delta^{13}C_{CO2}(\%)\right] = 100 \times \left(\left[\delta^{13}C_{CO2}(\%)\right](S) - \left[\delta^{13}C_{CO2}(\%)\right](I)\right) / \left[\delta^{13}C_{CO2}(\%)\right](I)(\%) \quad (8)$$

$$\Delta[pCO_2] = 100 \times ([pCO_2](S) - [pCO_2](I)) / [pCO_2](I)(\%) \quad (9)$$

where $\Delta[\delta^{13}C_{CO2}$ (‰)], and $\Delta[pCO_2]$ represent the % change of $\delta^{13}C_{CO2}$ (‰) and pCO_2 in depth-profiles and outflow waters compared with inflow waters, respectively.

2.5. Reservoir effect index

Upon the knowledge of CO_2 emission, we hypothesize and proposed that CO_2 emission is primarily related to the reservoir effect index (R_i, d m^{-1}), which serves as a metric to assess the effects of residence time and thermal characteristics on CO_2 emission. R_i is defined as:

$$R_i = \frac{HRT}{NWL}, \quad (10)$$

where HRT (days) is the hydraulic retention time of the reservoirs and NWL (m) refers to the normal water level of the reservoir.

2.6. Metadata compiling and established function between R_i and CO_2 emission

In addition to our studied sites, we searched published studies on CO_2 emission in reservoirs, and found more than 100 reservoirs (St. Louis *et al* 2000, Rosa *et al* 2004, Tremblay *et al* 2005, Dos Santos *et al* 2006, Guérin *et al* 2006, Barros *et al* 2011, Li *et al* 2015, Wen *et al* 2017). However, to investigate the relationship between CO_2 flux and R_i, only the sites which were documented simultaneously with reservoir morphometries (geographical locations, area) and CO_2 flux during the study year (more than two samples in non-frozen reservoirs and one sample in frozen reservoirs) were included. Consequently, 43 reservoirs from tropical to boreal areas were included and analyzed in this study. Specifically, there were 14 sites from Asia, 3 sites from Europe, 15 sites from North America, and 11 sites from South America (table S1).

The correlation of pCO_2, $\delta^{13}C_{CO2}$, average T_A, and CO_2 flux with the concerned environmental parameters in the studied reservoirs were analyzed using Pearson's correlation coefficient, and a one-way analysis of variance was conducted to analyze the differences. Besides, a t-test approach was used to compare the linear regression slopes. All the analyses were performed using the SPSS 19.0 statistical software package (SPSS Inc.) and the level of significance used was $P < 0.05$ was accepted as the level of significance.

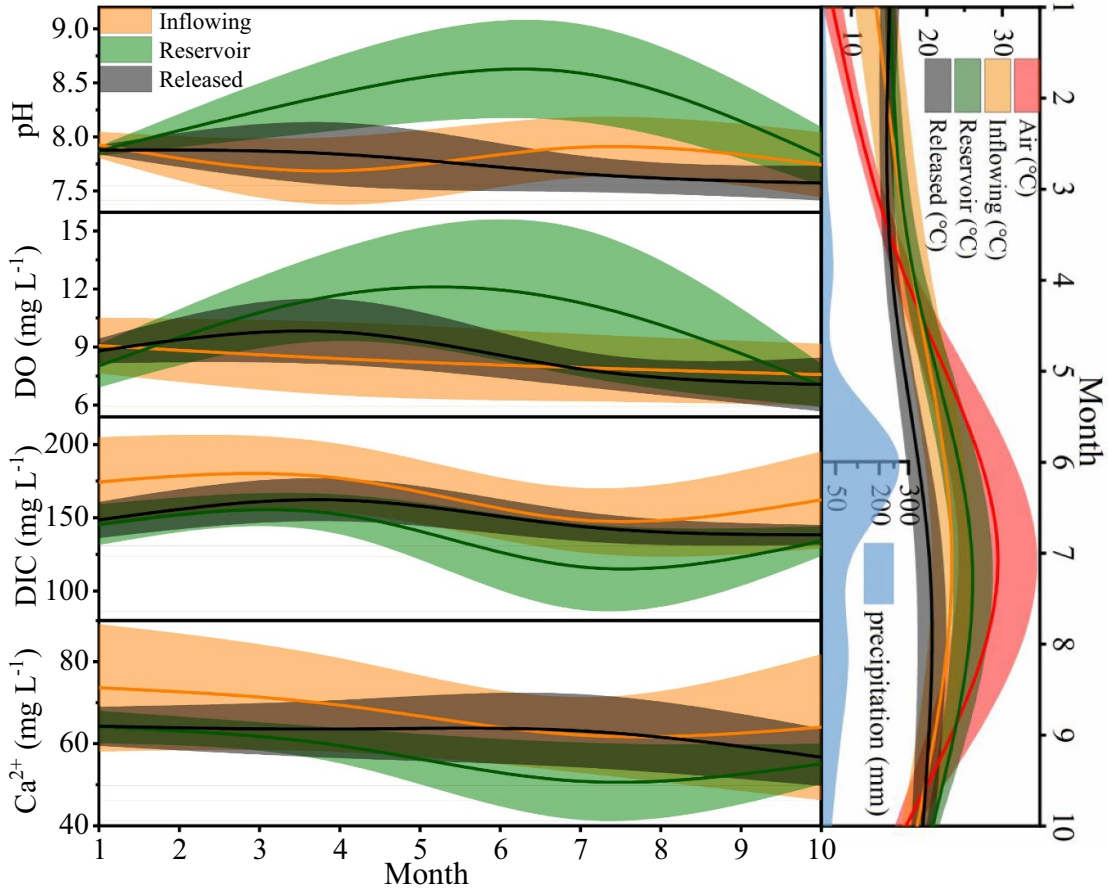

Figure 2. Temporal variations in air temperature, precipitation, water temperature, pH, dissolved oxygen, dissolved inorganic carbon, and Ca^{2+} in the reservoirs on the Wujiang River. The data are presented as mean ± standard error.

3. Results

3.1. Characteristics of meteorological and water chemical components

The average T_A were 16.6 °C and 19.6 °C in the upstream and downstream of the Wujiang River while the average precipitation was close in the two reaches (1068.3 mm and 1062.8 mm) (Gzpwrd 2017). Generally speaking, T_A, and precipitation during the warm season (April to September) were much higher than in the cold season (October to next March) (figure 2). The water temperature (T_W) varied seasonally ranging from 8.2 °C to 29.8 °C (mean = 18.0 °C, SD = 3.9), and T_W variations in the warm season was much larger than those in the cold season (table 2 and figure 2). In addition, T_W decreased markedly with depth in reservoirs (HF, HJD, DF, WJD, and SL) with an obvious thermal stratification and kept almost constant in the hypolimnion (figure 3). Similar to T_W, DO (mean = 7.6 mg l^{-1}, SD = 2.4), Chl (mean = 2.5 μg l^{-1}, SD = 4.4), and pH (mean = 7.9, SD = 0.3) declined with the increase of water depths. Unlike T_W, DIC (mean = 148.3 mg l^{-1}, SD = 21.1) and Ca^{2+} (mean = 60.4 mg l^{-1}, SD = 9.4) increased along the depth profile and the lowest and highest values appeared in the epilimnion of the warm season and hypolimnion in the cold season, respectively. The water chemical components had less variations with depth in the SFY, PS, and YP reservoirs (figure 3), where the seasonal thermal stratifications were weak due to shorter HRT.

3.2. Spatiotemporal patterns of pCO_2 and $\delta^{13}C_{CO2}$

Overall, pCO_2 in the Wujiang River had obvious spatiotemporal heterogeneity, ranging from 55.6 to 21 057.3 μatm (mean = 3205.7 μatm, SD = 2183.4) (figure 4(a)). The variations in pCO_2 in the warm season were obviously larger than those in the cold season, and the variations gradually lessened from upstream to downstream (table 2 and figure 4(a)). pCO_2 decreased in the order (released water > inflowing water > water in the reservoir) in all reservoirs except for the SL reservoir (table 2). Moreover, pCO_2 increased obviously along the vertical profiles (i.e. depth) at HF, HJD, DF, WJD, and SL reservoirs with longer HRT, while stabled at SFY, PS, and YP reservoirs with shorter HRT. In this study, the highest pCO_2 (21 057.3 μatm) in the hypolimnion and the lowest values (55.6 μatm) in the epilimnion were all recorded in the warm season of the SL reservoir.

$\delta^{13}C_{CO2}$ changed from −22.5‰ to −10.7‰ (mean = −18.9‰, SD = 1.6) (figure 4(a)). Similar to

Table 2. Water chemical parameters of the studied reservoirs on the Wujiang River, Southwest China[a].

Parameters	Inflowing[b] ($n = 68$)	HF ($n = 50$)	HJD ($n = 64$)	DF ($n = 40$)	SFY ($n = 20$)	WJD ($n = 72$)	SL ($n = 48$)	PS ($n = 48$)	YP ($n = 20$)	Released water ($n = 28$)
T_W (°C)	18.40 ± 4.34	17.73 ± 5.40	16.73 ± 3.77	16.95 ± 3.52	17.20 ± 2.67	18.40 ± 3.63	19.10 ± 3.64	18.84 ± 2.77	18.95 ± 2.89	17.59 ± 2.73
pH[d]	7.90 ± 0.28	8.17 ± 0.38	7.83 ± 0.27	7.93 ± 0.29	7.76 ± 0.78	7.85 ± 0.25	8.15 ± 0.47	7.81 ± 0.15	7.82 ± 0.16	7.75 ± 0.22
DO ($mg\,l^{-1}$)	8.25 ± 1.73	6.23 ± 3.45	6.63 ± 1.91	8.35 ± 1.93	7.90 ± 1.27	7.63 ± 2.64	6.78 ± 3.46	8.29 ± 0.72	8.39 ± 0.63	8.38 ± 1.55
DO (%)	93.13 ± 20.56	65.25 ± 38.8	78.02 ± 24.97	96.93 ± 28.4	89.94 ± 14.89	88.63 ± 32.69	77.31 ± 46.25	91.49 ± 8.84	91.92 ± 6.69	93.96 ± 16.2
DIC ($mg\,l^{-1}$)	165.52 ± 29.3	143.6 ± 19.25	134.48 ± 17.33	135.08 ± 12.21	144.54 ± 15.1	143.41 ± 10.7	161.37 ± 16.96	153.68 ± 11.5	145.81 ± 6.48	148.29 ± 13.9
Chl ($\mu g\,l^{-1}$)	2.84 ± 5.51	5.35 ± 3.60	1.28 ± 1.90	2.90 ± 5.59	1.74 ± 3.53	3.88 ± 5.78	2.61 ± 4.57	0.97 ± 0.75	0.37 ± 0.25	0.78 ± 0.59
Ca^{2+} ($mg\,l^{-1}$)	67.29 ± 14.33	48.82 ± 6.23	60.30 ± 6.87	61.53 ± 7.71	63.87 ± 4.48	63.86 ± 3.41	63.24 ± 6.86	55.36 ± 2.38	52.86 ± 3.69	61.93 ± 7.35
pCO_2 (10^3 μatm)	3.51 ± 3.33	2.23 ± 1.73	3.08 ± 1.58	2.78 ± 1.51	3.21 ± 1.89	3.09 ± 1.49	4.88 ± 2.87	2.86 ± 1.01	2.68 ± 1.03	3.57 ± 2.1
$\delta^{13}C_{DIC}$ (‰)	−9.2 ± 1.3	−7.5 ± 2.0	−8.5 ± 1.8	−8.9 ± 1.5	−9.3 ± 0.7	−9.2 ± 0.9	−9.9 ± 1.1	−10.3 ± 0.7	−10.4 ± 0.6	−9.9 ± 0.7
$\delta^{13}C_{CO2}$ (‰)	−18.9 ± 1.3	−17.2 ± 2.0	−18.4 ± 2.1	−18.7 ± 1.8	−19.1 ± 0.6	−18.8 ± 1.2	−19.4 ± 1.4	−19.9 ± 0.7	−20.0 ± 0.7	−19.6 ± 0.6

[a] The data are presented as the mean ± standard error; n is the number of measurements. The sampling sites were divided into three categories: inflowing water, released water, and reservoir water of the eight reservoirs.

[b] Inflowing: the water that was from the stations in the reservoir sections that directly received river inflows and the sites in the tributaries.

[c] HRT is hydraulic retention time.

[d] Average pH is calculated geometrically.

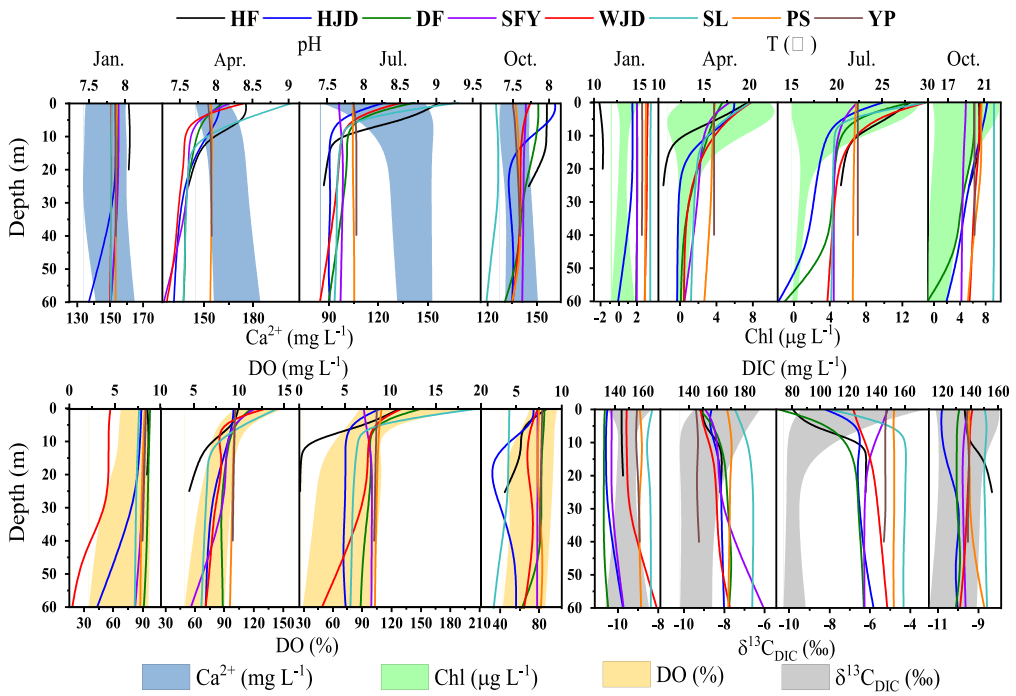

Figure 3. Depth profiles of pH, T, DO, DIC, Ca^{2+}, Chl, DO (%), and $\delta^{13}C_{DIC}$ in the eight reservoirs. The data of pH, T, DO, and DIC are symbolized by the solid lines. The values of Ca^{2+}, Chl, DO (%), and $\delta^{13}C_{DIC}$ are presented as mean ± standard error.

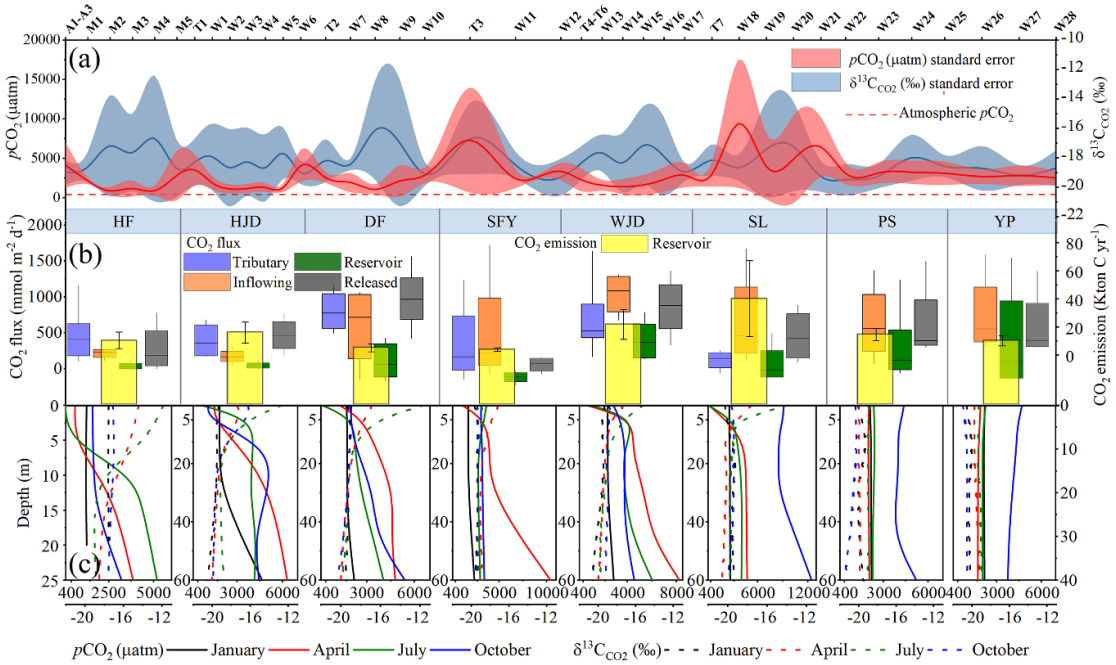

Figure 4. (a) Variations in pCO_2 in the surface water of the reservoirs on the Wujang River. The data are presented as mean ± standard error. (b) Variations in the CO_2 fluxes and emissions in the reservoirs on the Wujiang River. For the CO_2 flux data, the boxes and whiskers indicate the 25th to 75th and 10th and 90th percentiles, respectively. The central lines indicate the median and the outliers are not included. The data for the CO_2 emissions are presented as mean ± standard error. (c) Depth profiles of pCO_2 and $\delta^{13}C_{CO2}$ (‰) in the reservoirs on the Wujiang River. The name abbreviations of each reservoir refer to figure 1.

pCO_2, the variations of $\delta^{13}C_{CO2}$ in the warm season were larger than those in the cold season. However, different from pCO_2, $\delta^{13}C_{CO2}$ decreased from the upstream to the downstream (table 2 and figure 4(a)). $\delta^{13}C_{CO2}$ values varied between reservoirs, ranged from −20.5‰ to −10.7‰ (mean = −18.4‰, SD = 2.1) in the HJD reservoir with the longest HRT. Whereas $\delta^{13}C_{CO2}$ ranged from −21.0‰ to −19.0‰ (mean = −20.0‰, SD = 0.7) in the YP reservoir with the shortest HRT. The highest (−10.7‰) and lowest

values (−22.4‰) of $\delta^{13}C_{CO2}$ were recorded in multi-year regulated reservoirs of HJD and HF, respectively.

3.3. Amounts of CO_2 flux and CO_2 emission

CO_2 fluxes from all the studied sites ranged from −9.0 mmol m^{-2} d^{-1} to 2269.3 mmol m^{-2} d^{-1} (mean = 260.1 mmol m^{-2} d^{-1}, SD = 314.1). In the SFY, PS, and YP reservoirs with short HRT, there was no discernable difference in CO_2 flux between the reservoir water and released water (figure 4(b) and table 2). However, in the HF, HJD, DF, WJD, and SL reservoirs with longer HRT, CO_2 fluxes in released water were larger than those in reservoir water. In particular, the HJD reservoir showed a large difference in CO_2 flux between released water (469.8 mmol m^{-2} d^{-1}) and reservoir water (46.8 mmol m^{-2} d^{-1}), more than 10 times (figure 4(b)). In addition, the highest (240.6 mmol m^{-2} d^{-1}) and the lowest (42.5 mmol m^{-2} d^{-1}) mean CO_2 flux were observed in the SL and HF reservoirs, respectively.

The total CO_2 emission from the reservoirs was 1.25 × 10^5 ton CO_2-C y^{-1}. Notably, CO_2 emissions from HJD, WJD, SL, and PS reservoirs (1.49 × 10^4 ton CO_2-C y^{-1} to 4.04 × 10^5 ton CO_2-C y^{-1}) were significant higher than these from HF, DF, SFY, and YP reservoirs (4.18 × 10^3 ton CO_2-C y^{-1} to 1.06 × 10^4 ton CO_2-C y^{-1}) (figure 4(b)). Moreover, the largest CO_2 emissions (4.04 × 10^5 ton CO_2-C y^{-1}) appeared in SL reservoir, which was nearly 10 times and 4 times higher than the daily-regulated reservoirs of SFY (upstream) and YP (downstream).

4. Discussion

4.1. CO_2 production impacted by biogeochemical processes in the reservoirs

Previous studies have reported that the river damming can capture suspended particles and lead to large accumulation of organic carbon (OC), suggesting that the high concentration of CO_2 in reservoirs is more likely to be controlled by OC mineralization (St. Louis *et al* 2000, Abril *et al* 2005, Li *et al* 2018b, Wang *et al* 2019b). However, CO_2 production is more complicated because pCO_2 showed seasonal variation in karst cascade reservoir system (Pu *et al* 2020, Wang *et al* 2020b). Our study based on the multiple regression analysis suggested that pH and DO were the dominant indicator parameters for tracing CO_2 characteristics in the inflowing and released water (table 3). However, the results also suggested that CO_2 production in karst cascade reservoirs may be influenced by multiple influence factors (table 3). It is hence important to understand the damming effect on carbon cycle by comparing the differences between reservoir water and inflowing water (Goudie and Viles 2012, Wang *et al* 2020a). Moreover, variations in CO_2 concentration and $\delta^{13}C_{CO2}$ signature in the waters can indicate complicated processes (Maberly *et al* 2012). To parse out the relative importance of various biogeochemical processes on CO_2 production, we resorted to $\Delta[pCO_2]$ and $\Delta[\delta^{13}C_{CO2}]$, which theoretically follows a strong quadratic relationship (figure 5(a)). All plausible biogeochemical processes were then applied to decipher the quadratic relationship between $\Delta[pCO_2]$ and $\Delta[\delta^{13}C_{CO2}]$ as further explained as below.

4.2. CO_2 dynamics in the reservoirs with relatively long hydraulic residence time

The reservoirs with long HRT were prone to develop strong thermal stratification in the warm season; this provide a favorable environment for phytoplankton growth and was thus responsible for the higher Chl concentration in reservoirs (figure 3) (Li *et al* 2018b, Yang *et al* 2020, Wang *et al* 2020a). We proposed that phytoplankton photosynthesis and assimilation the light C isotopes (^{12}C) of CO_2 (aq) as C source led to depletion of CO_2 and ^{13}C enrichment of residual inorganic C in the epilimnion (Van Breugel *et al* 2005, Doctor *et al* 2008). This is supported by the significant correlation between Chl concentration with pCO_2 and $\delta^{13}C_{CO2}$ where CO_2 was mainly consumed by phytoplankton photosynthesis (table 3). Thus, the above-mentioned two processes would lead to a decrease of both $\Delta[pCO_2]$ and $\Delta[\delta^{13}C_{CO2}]$ in the epilimnion (figure 5(a)). Moreover, due to the biological production, pH increase obviously in the epilimnion, which increase water supersaturation coefficient and accelerate the secondary carbonate precipitation (Van Breugel *et al* 2005, Pu *et al* 2020). The Ca^{2+} concentration and pCO_2 decreased markedly in the epilimnion and the positive correlation between Ca^{2+} and pCO_2 confirms carbonate precipitation (figure 3 and table 3).

In the thermocline and hypolimnion, DO, pH and $\delta^{13}C_{CO2}$ decreased, while pCO_2 and Ca^{2+} increased markedly, indicating that OM degradation is the dominant process that accelerates the carbonate dissolution (Wang *et al* 2019b, Binet *et al* 2020). In July, from epilimnion to hypolimnion, Ca^{2+} in HF and HJD reservoirs increased by 69.75% (33.6 mg l^{-1} to 40.1 mg l^{-1}) and 35.30% (46.3 mg l^{-1} to 62.7 mg l^{-1}), respectively. This further proved that the dissolution rate of carbonate was accelerated in the hypolimnion (Pu *et al* 2020, Wang *et al* 2020b). In addition, thermal stratification would seriously hinder water exchange in the column (Encinas Fernandez *et al* 2014), which caused high pCO_2 in the hypolimnion and be responsible for the high values of $\Delta[pCO_2]$ and $\Delta[\delta^{13}C_{CO2}]$ in released water (figures 4 and 5) (Goudie and Viles 2012, Binet *et al* 2020). Moreover, pCO_2 was maintained at a high level due to the released water with lower pH and the process of oxygen input, which further accelerated OM degradation and carbonate dissolution (figure 4(c)) (Tranvik *et al* 2009). Regarding the epilimnion, in the cold

Table 3. The correlation of pCO_2 and $\delta^{13}C_{CO2}$ (‰) with the concerned environmental parameters in the studied reservoirs on Wujiang River[a].

	Inflowing			Reservoir			Released water		
	r^2	P	n	r^2	P	n	r^2	P	n
T_W (°C)	0.039/0.143	0.749/0.244	68	−0.89/0.383[b]	0.091/< 0.001	362	0.261/−0.097	0.180/0.623	28
pH	−0.827[b]/0.444[b]	< 0.001/< 0.001	68	−0.843[b]/0.725[b]	< 0.001/< 0.001	362	−0.913[b]/0.091	< 0.001/0.645	28
DO (mg l^{-1})	−0.458[b]/0.361[b]	< 0.001/0.003	68	−0.631[b]/0.439[b]	< 0.001/< 0.001	362	−0.646[b]/0.290	< 0.001/0.135	28
Chl (μg l^{-1})	−0.086/0.417[b]	0.493/< 0.001	68	−0.336[b]/0.554[b]	< 0.001/< 0.001	362	0.402/−0.142	0.034/0.472	28
DIC (mg l^{-1})	0.304[c]/−0.159	0.012/0.196	68	0.309[b]/−0.466[b]	< 0.001/< 0.001	362	0.237/−0.124	0.226/0.531	28
Ca^{2+} (mg l^{-1})	−0.017/0.222	0.890/0.068	68	0.352[b]/−0.490[b]	< 0.001/< 0.001	362	0.261/0.325	0.180/0.092	28

[a] n is the number of samples, while P is the significance level.

[b] The correlation was significant at the 0.01 level.

[c] The correlation was significant at the 0.05 level.

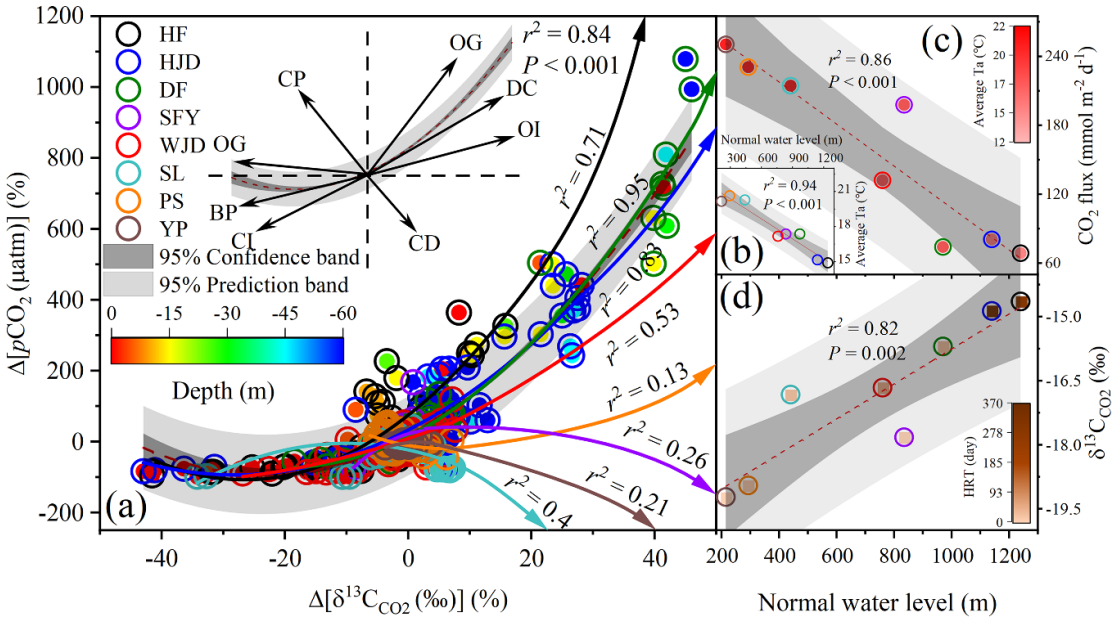

Figure 5. (a) $\Delta[pCO_2](\%)$ versus the $\Delta[\delta^{13}C_{CO2}](\%)$. The data consist of each reservoir is symbolized by the hollow color circles and depth (m) is symbolized by the solid color circles. CP (carbonate precipitation), OG (outgassing of CO_2), BP (biological production), CI (CO_2 input), CD (carbonate dissolution), OI (oxygen input), and DC (degradation of carbon) represent the different processes affecting CO_2 flux; (b) average T_A versus the normal water level; (c) CO_2 flux versus the normal water level and (d) $\delta^{13}C_{CO2}$ versus the normal water level. The data consist of the means of each reservoir is symbolized by the hollow color circles. Average T_A and hydraulic retention time (HRT) are symbolized by the solid color circles.

season, pCO_2 was significantly higher but $\delta^{13}C_{CO2}$ was lower than that in the warm season, indicating that the decrease in atmospheric temperature led to weak thermal stratification (Boehrer and Schultze 2008, López Bellido *et al* 2009), which enhanced the hydrodynamics condition. Consequently, the biological effect was inhibited and CO_2 was released from the hypolimnion (figure 3) (Borges *et al* 2012). Thus, the source of CO_2 is mainly controlled by the degradation of OM and carbonate dissolution in the cold season.

4.3. CO_2 dynamics in the reservoirs with relatively shorter hydraulic residence time

In the SFY, PS, and YP reservoirs with relative shorter HRT, there was no obvious thermal stratification all year due to the strong hydrodynamics (figure 3). However, the $\delta^{13}C_{CO2}$ in the downstream is larger than the upstream, indicating that the higher air temperature may accelerate OM degradation in the downstream (table 2 and figure 4(a)) (Maberly *et al* 2012). In this study, SL reservoir is the only reservoir with seasonal thermal stratification in the downstream (figure 3). Although the HRT of SL reservoir (22 d) was shorter than those of HJD (368 d), HF (302 d), DF (29 d) and WJD (49 d) reservoirs in the upstream, the lower mean value of $\delta^{13}C_{CO2}$ (−19.4‰) and higher pCO_2 (4878.0 μatm) appeared in SL reservoir, which may indicate that the thermal stratification of water became weaker in the cold season and this accelerated OM degradation and was responsible for the higher pCO_2 and lower $\delta^{13}C_{CO2}$ at higher air temperatures (mean = 20.3 °C) in the downstream (figure 4(a)). However, in the downstream of SL reservoir, pCO_2 remained stable in PS and YP reservoirs, indicating that the cumulative damming effect on carbon is not significant in cascade reservoirs. In the reservoirs with shorter HRT, the thermal stratification was weak and water chemical characteristics were similar to river system. Thus, our results suggest that CO_2 production in the riverine area was mainly influenced by the carbonate weathering and degradation of OM (Chen *et al* 2020, Zhong *et al* 2020, Yi *et al* 2021), while was also gradually affected by the multiple processes including, carbonate dissolution and precipitation, biological production, OM degradation, CO_2 outgassing and oxygen input in the karst river-reservoir system (figures 5(a) and 6). In conclusion, the damming effect on carbon cycle is significantly smaller in the reservoirs with short HRT of daily and weekly regulation than in the reservoirs with long HRT of monthly and annual regulation. This is mainly because that even if the air temperature is high, the reservoir water is difficult to form stable thermal stratification due to strong hydrodynamic force in the reservoirs with short HRT. Therefore, reservoir manager could reduce negative damming effects by adjusting the HRT.

4.4. Environmental factors control of the CO_2 flux in the cascade reservoirs

The CO_2 flux is influenced by multiple environmental factors such as reservoir age (St. Louis *et al* 2000,

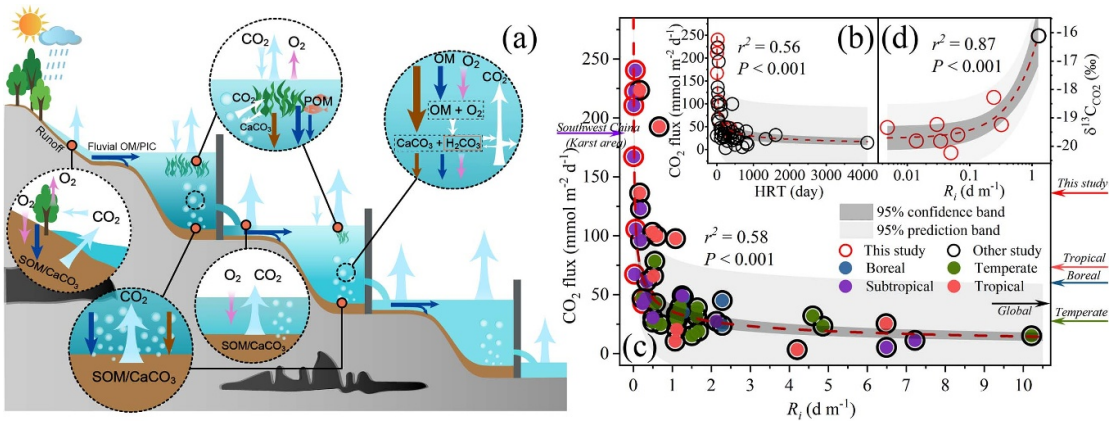

Figure 6. (a) Main processes affecting CO_2 emissions from karst cascade reservoir; (b) CO_2 flux versus the reservoir effect index (R_i), (c) CO_2 flux versus the hydraulic retention time (HRT), and (d) $\delta^{13}C_{CO2}$ versus the R_i. The data consist of the means in each reservoir and in each climate region and they are symbolized by the hollow color circles and solid color circles, respectively. The correlation regressions are as follows: (b) $y = 428.31x^{-0.446}$, adjusted $r^2 = 0.56$, $P < 0.001$; (c) $y = 37.232x^{-0.444}$, adjusted $r^2 = 0.58$; (d) $y = -19.719 + 2.877x$, adjusted $r^2 = 0.87$, $P < 0.001$. The reservoir effect index (R_i) was Log10 transformed in (d). The complete lists of the reservoir CO_2 fluxes and the hydrological parameters from other works are given in table S1. The arrows in different colors represent the average CO_2 flux in different region.

Sobek *et al* 2005, Barros *et al* 2011, Binet *et al* 2020), air temperature (Sobek *et al* 2005, Binet *et al* 2020), HRT (Wang *et al* 2015, Catalán *et al* 2016, Li *et al* 2018a, Kumar *et al* 2019), water depth (Yang *et al* 2020), windspeed (Richey *et al* 2002, Borges *et al* 2012), latitude (Barros *et al* 2011, Li 2018c) and so on. In cascade reservoirs, the formation of thermal stratification, which is mainly controlled by the T_A and HRT, can influence the water depth, reservoir area, physiology of organisms and carbon cycle (Boehrer and Schultze 2008, Barros *et al* 2011, Wang *et al* 2015, 2020a, Catalán *et al* 2016, Xiao *et al* 2021). In this study, with the decrease of altitude from upstream to downstream, air temperature increased obviously (table 1 and figure 5(b)). Moreover, three were significant relationships between NWL with the CO_2 flux (significant negative relationship) and $\delta^{13}C_{CO2}$ (significant positive correlation) (figures 5(c) and (d)). It is suggested that with the decrease of NWL in the downstream, higher air and water temperatures accelerated OM degradation and were responsible for the high CO_2 fluxes (Tranvik *et al* 2009). The CO_2 fluxes in HJD and HF reservoirs (longer HRT and higher NWL) were markedly lower than those in PS and YP reservoirs (shorter HRT and lower NWL), indicating the accelerated OM degradation in the downstream (table 2 and figure 4(b)). Since the reservoir water is discharged at the bottom of the dam, the released water from the hypolimnion is responsible for the higher CO_2 fluxes (Goudie and Viles 2012, Li *et al* 2018a). Although HJD reservoir had the longest HRT, CO_2 fluxes in HJD reservoir (mean = 81.3 mmol m^{-2} d^{-1}) was obviously lower than those in SL reservoir (mean = 216.2 mmol m^{-2} d^{-1}). This indicates that under the condition of lower NWL, higher air temperature and obvious thermal stratification can enhance the accumulation of CO_2 in the hypolimnion and enhance the CO_2 emission in the released water. Thus, our study suggests that NWL and HRT are two important parameters for jointly controlling CO_2 fluxes in the reservoir area and released water.

Although CO_2 fluxes in the released water were higher, the reservoir surface area increased dramatically after the damming, leading to that overall amount of CO_2 emission in reservoir was larger than that in the released water (Abril *et al* 2005). Abril *et al* (2005) and Wang *et al* (2019a) suggested that the total CO_2 emissions from the reservoir area is nearly 10 times larger than the emission from released water. Therefore, previous studies mainly focused on CO_2 emissions from the reservoir area (Deemer *et al* 2016, Kumar *et al* 2019, Wang *et al* 2019b). Given the control of the hydrological and geographical factors for CO_2 emissions observed in this study, the CO_2 fluxes and reservoir effect index (R_i) from the other reservoirs around the world were collected from the references (table S1). In our studied eight karst reservoirs, R_i and CO_2 fluxes were ranged from 0.005 to 0.3 d m^{-1} (mean = 0.1, SD = 0.1) and 42.5 to 240.6 mmol m^{-2} d^{-1} (mean = 137.9 mmol m^{-2} d^{-1}, SD = 82.2) in this study and were ranged from 0.005 to 10.2 d m^{-1} (mean = 1.6, SD = 2.1) and 3.4 to 223.6 mmol m^{-2} d^{-1} (mean = 52.1 mmol m^{-2} d^{-1}, SD = 47.1) in all reservoirs. Both R_i and CO_2 fluxes showed significant spatial variation. Mean CO_2 fluxes in the eight karst reservoirs are similar to the results in other karst reservoirs, but they are much larger than those in non-karst reservoirs (table S1) (Wen *et al* 2017, Pu *et al* 2019). The significant relationship between HRT and CO_2 flux further proved that HRT is an important factor affecting the CO_2 flux (figure 6(b)) (Wang *et al* 2015, Li *et al* 2018a). In addition, R_i which is constrained by both of the HRT and

NWL also showed a significant correlation with CO_2 flux. Since the x-coordinate data defined by R_i are mainly concentrated in the range of 0–1. R_i can better indicate the CO_2 fluxes in the surface of reservoirs (figure 6(c)). Besides, the significant positive relationship between R_i and $\delta^{13}C_{CO2}$ further indicates that the damming effect has significantly affected the characteristics and flux of CO_2 (figure 6(d)). Compared with HRT, R_i would be a better index to predict the CO_2 flux in reservoirs. Thus, the empirical relationship between the CO_2 flux and R_i will help to evaluate the reservoir CO_2 flux and carbon budget in a large spatial scale since the R_i is more easily accessed than CO_2 flux.

As discussed above, in the reservoirs with longer HRT and lower NWL, CO_2 emissions was much larger (figure 4(b)). Moreover, although the HRT in WJD and SL reservoirs in the middle and lower reaches were much shorter than those in HF, HJD, and DF reservoirs in the upstream, the CO_2 emissions in WJD and SL reservoirs were much higher (figure 4(b)). In addition, although the air temperatures in PS and YP reservoirs were higher, there was no obvious thermal stratification in these two reservoirs due to short HRT. CO_2 emissions in PS and YP reservoirs were much lower than those in HF and HJD reservoir with higher NWL and longer HRT. The results indicate that the reduction of HRT by artificial regulation can reduce CO_2 emissions effectively, particularly playing an important role in reservoirs with lower altitude. Thus, our study suggested that government and scientists could consider coupling of the hydrodynamics of reservoir and biogeochemical cycling to improve reservoir management. This is because that once these reservoirs form stable thermal stratification in lentic zone, damming effect on the carbon cycle may be stronger than reservoirs with lower temperatures and longer HRT. Artificial regulation could effectively weaken the side effect on carbon transport and transformation, especially in the cascade reservoirs.

5. Conclusion

To conclude, this study reveals the control mechanism and environmental impact of CO_2 production in cascade reservoirs by fitting the $\Delta[pCO_2]$ and $\Delta[\delta^{13}C_{CO2}(‰)]$. The reservoir CO_2 fluxes (240.6 mmol m^{-2} d^{-1}) and emissions (40.4 ton CO_2-C y^{-1}) in SL reservoir (with higher HRT and lower NWL) are markedly higher than the average value of the eight cascade reservoirs (137.9 mmol m^{-2} d^{-1}, 15.6 ton CO_2-C y^{-1}). Moreover, $\delta^{13}C_{CO2}(‰)$ varied largely from −20.6‰ to −13.6‰ in SL reservoir, indicating that HRT and NWL are important environmental factors for controlling CO_2 flux. Thus, the relationships between the R_i (HRT/NWL) and CO_2 production/emissions are crucial to estimate the carbon dynamics and budget accurately at riverine system in regional and global scale. The estimation of CO_2 dynamics in reservoirs would provide hints to optimize reservoirs management for environmental and ecological needs. Overall, our study not only enriches the understanding of the regulation of the hydrologic regime for CO_2 production and emissions in cascade reservoirs but also further provides theoretical support for the reservoir regulation to reduce CO_2 emissions.

Data availability statement

The data that support the findings of this study are available from the corresponding author upon reasonable request.

All data that support the findings of this study are included within the article (and any supplementary files).

Acknowledgments

This work was supported by the National Key R&D Program of China (Grant No. 2016YFA0601002), National Natural Science Foundation of China (Grant No. 41925002), and Tianjin Research Innovation Project for Postgraduate Students (Grant No. 2019YJSB183). We thank the kind help of our team in the fieldwork.

ORCID iD

Wanfa Wang https://orcid.org/0000-0001-8835-9808

References

Abril G, Guérin F, Richard S, Delmas R, Galy-Lacaux C, Gosse P, Tremblay A, Varfalvy L, Dos Santos M A and Matvienko B 2005 Carbon dioxide and methane emissions and the carbon budget of a 10 year old tropical reservoir (Petit Saut, French Guiana) *Glob. Biogeochem. Cycles* **19** GB4007

Barros N, Cole J J, Tranvik L J, Prairie Y T, Bastviken D, Huszar V L, Del Giorgio P and Roland F 2011 Carbon emission from hydroelectric reservoirs linked to reservoir age and latitude *Nat. Geosci.* **4** 593

Beaulieu E, Goddéris Y, Donnadieu Y, Labat D and Roelandt C 2012 High sensitivity of the continental-weathering carbon dioxide sink to future climate change *Nat. Clim. Change* **2** 346–9

Binet S, Probst J L, Batiot C, Seidel J L, Emblanch C, Peyraube N, Charlier J B, Bakalowicz M and Probst A 2020 Global warming and acid atmospheric deposition impacts on carbonate dissolution and CO_2 fluxes in French karst hydrosystems: evidence from hydrochemical monitoring in recent decades *Geochim. Cosmochim. Acta* **270** 184–200

Boehrer B and Schultze M 2008 Stratification of lakes *Rev. Geophys.* **46** RG2005

Borges A V *et al* 2012 *Variability of Carbon Dioxide and Methane in the Epilimnion of Lake Kivu* (Berlin: Springer) pp 47–66

Butman D and Raymond P A 2011 Significant efflux of carbon dioxide from streams and rivers in the United States *Nat. Geosci.* **4** 839–42

Catalán N, Marcé R, Kothawala D N and Tranvik L J 2016 Organic carbon decomposition rates controlled by water retention time across inland waters *Nat. Geosci.* **9** 501–4

Chen S N, Yue F J, Liu X L, Zhong J, Yi Y B, Wang W F, Qi Y, Xiao H Y and Li S L 2021 Seasonal variation of nitrogen biogeochemical processes constrained by nitrate dual isotopes in cascade reservoirs, Southwestern China *Environ. Sci. Pollut. Res.* (https://doi.org/10.1007/s11356-021-12505-9)

Chen S, Zhong J, Li C, Liu J, Wang W F, Xu S and Li S L 2020 Coupled effects of hydrology and temperature on temporal dynamics of dissolved carbon in the Min River, Tibetan Plateau *J. Hydrol.* **593** 125641

Clark I D and Fritz P 1997 *Environmental Isotopes in Hydrogeology* (New York: Lewis Publishers)

Cole J J *et al* 2007 Plumbing the global carbon cycle: integrating inland waters into the terrestrial carbon budget *Ecosystems* **10** 171–84

Cole J J and Caraco N F 1998 Atmospheric exchange of carbon dioxide in a low-wind oligotrophic lake measured by the addition of SF6 *Limnol. Oceanogr.* **43** 647–56

Deemer B R, Harrison J A, Li S, Beaulieu J J, DelSontro T, Barros N, Bezerra-Neto J F, Powers S M, Dos Santos M A and Vonk J A 2016 Greenhouse gas emissions from reservoir water surfaces: a new global synthesis *BioScience* **66** 949–64

Doctor D H, Kendall C, Sebestyen S D, Shanley J B, Ohte N and Boyer E W 2008 Carbon isotope fractionation of dissolved inorganic carbon (DIC) due to outgassing of carbon dioxide from a headwater stream *Hydrol. Process.* **22** 2410–23

Dos Santos M A, Rosa L P, Sikar B, Sikar E and Dos Santos E O 2006 Gross greenhouse gas fluxes from hydro-power reservoir compared to thermo-power plants *Energy Policy* **34** 481–8

EBHHC 2007 *The History of Hydroelectricity in China 1904 ~ 2000* (Beijing: China Waterpower Press)

Encinas Fernandez J, Peeters F and Hofmann H 2014 Importance of the autumn overturn and anoxic conditions in the hypolimnion for the annual methane emissions from a temperate lake *Environ. Sci. Technol.* **48** 7297–304

Ford D and Williams P 2007 *Karst Hydrogeology and Geomorphology* (New York: Wiley)

Gaillardet J, Dupré B, Louvat P I and Allegre C J 1999 Global silicate weathering and CO_2 consumption rates deduced from the chemistry of large rivers *Chem. Geol.* **159** 3–30

Gibson L, Wilman E N and Laurance W F 2017 How green is 'green' energy? *Trends Ecol. Evol.* **32** 922–35

Goudie A S and Viles H A 2012 Weathering and the global carbon cycle: geomorphological perspectives *Earth Sci. Rev.* **113** 59–71

Grill G *et al* 2019 Mapping the world's free-flowing rivers *Nature* **569** 215–21

Grill G, Lehner B, Lumsdon A E, MacDonald G K, Zarfl C and Reidy Liermann C 2015 An index-based framework for assessing patterns and trends in river fragmentation and flow regulation by global dams at multiple scales *Environ. Res. Lett.* **10** 015001

Guérin F, Abril G, Richard S, Burban B, Reynouard C, Seyler P and Delmas R 2006 Methane and carbon dioxide emissions from tropical reservoirs: significance of downstream rivers *Geophys. Res. Lett.* **33** L21407

Gzpwrd 2017 Water Resources Bulletin of Guizhou Province (available at: www.gzmwr.gov.cn/) (Accessed 15 January 2019) (in chinese)

Harned H S and Davis R 1943 The ionization constant of carbonic acid in water and the solubility of carbon dioxide in water and aqueous salt solutions from 0 to 50 *J. Am. Chem. Soc.* **65** 2030–7

Huttunen J T, Alm J, Liikanen A, Juutinen S, Larmola T, Hammar T, Silvola J and Martikainen P J 2003 Fluxes of methane, carbon dioxide and nitrous oxide in boreal lakes and potential anthropogenic effects on the aquatic greenhouse gas emissions *Chemosphere* **52** 609–21

ICOLD 2018 Number of dams by country members International Commission on Large Dams (World Register of Dams)

Jähne B, Heinz G and Dietrich W 1987 Measurement of the diffusion coefficients of sparingly soluble gases in water *J. Geophys. Res.* **92** 10767–76

Kumar A, Yang T and Sharma M P 2019 Greenhouse gas measurement from Chinese freshwater bodies: a review *J. Clean. Prod.* **233** 368–78

Li S Y 2018c CO_2 oversaturation and degassing using chambers and a new gas transfer velocity model from the Three Gorges Reservoir surface *Sci. Total Environ.* **640–641** 908–20

Li S Y, Bush R T, Santos I R, Zhang Q F, Song K S, Mao R, Wen Z D and Lu X X 2018b Large greenhouse gases emissions from China's lakes and reservoirs *Water Res.* **147** 13–24

Li S Y, Zhang Q F, Bush R T and Sullivan L A 2015 Methane and CO_2 emissions from China's hydroelectric reservoirs: a new quantitative synthesis *Environ. Sci. Pollut. Res.* **22** 5325–39

Li S, Wang F S, Zhou T, Cheng T Y and Wang B L 2018a Carbon dioxide emissions from cascade hydropower reservoirs along the Wujiang River, China *Inland Waters* **8** 157–66

Liang X, Xing T, Li J X, Wang B L, Wang F S, He C Q, Hou L J and Li S L 2019 Control of the hydraulic load on nitrous oxide emissions from cascade reservoirs *Environ. Sci. Technol.* **53** 11745–54

López Bellido J, Tulonen T, Kankaala P and Ojala A 2009 CO_2 and CH_4 fluxes during spring and autumn mixing periods in a boreal lake (Pääjärvi, southern Finland) *J. Geophys. Res.* **114** G04007

Maavara T, Chen Q W, Van Meter K, Brown L E, Zhang J Y, Ni J R and Zarfl C 2020 River dam impacts on biogeochemical cycling *Nat. Rev. Earth Environ.* **1** 103–16

Maberly S C, Barker P A, Stott A W and De Ville M M 2012 Catchment productivity controls CO_2 emissions from lakes *Nat. Clim. Change* **3** 391–4

Meybeck M 2003 Global occurrence of major elements in rivers *Treatise Geochem.* **5** 207–23

Mook W G, Bommerson J C and Staverman W H 1974 Carbon isotope fractionation between dissolved bicarbonate and gaseous carbon dioxide *Earth Planet. Sci. Lett.* **22** 169–76

Pu J B, Li J H, Zhang T, Martin J B, Khadka M B and Yuan D X 2019 Diel-scale variation of dissolved inorganic carbon during a rainfall event in a small karst stream in southern China *Environ. Sci. Pollut. Res.* **26** 11029–41

Pu J B, Li J H, Zhang T, Martin J B and Yuan D X 2020 Varying thermal structure controls the dynamics of CO_2 emissions from a subtropical reservoir, south China *Water Res.* **178** 115831

Räsänen T A, Varis O, Scherer L and Kummu M 2018 Greenhouse gas emissions of hydropower in the Mekong River Basin *Environ. Res. Lett.* **13** 034030

Rau G H, Riebesell U and Wolf-Gladrow D 1996 A model of photosynthetic ^{13}C fractionation by marine phytoplankton based on diffusive molecular CO_2 uptake *Mar. Ecol. Prog. Ser.* **133** 275–85

Raymond P A, Hartmann J, Lauerwald R, Sobek S, McDonald C, Hoover M, Butman D, Striegl R, Mayorga E and Humborg C 2013 Global carbon dioxide emissions from inland waters *Nature* **503** 355–9

Raymond P A, Zappa C J, Butman D, Bott T L, Potter J, Mulholland P, Laursen A E, McDowell W H and Newbold D 2012 Scaling the gas transfer velocity and hydraulic geometry in streams and small rivers *Limnol. Oceanogr. Fluids Environ.* **2** 41–53

Richey J E, Melack J M, Aufdenkampe A K, Ballester V M and Hess L L 2002 Outgassing from Amazonian rivers and wetlands as a large tropical source of atmospheric CO_2 *Nature* **416** 617–20

Rosa L P, Dos Santos M A, Matvienko B, Dos Santos E O and Sikar E 2004 Greenhouse gas emissions from hydroelectric reservoirs in tropical regions *Clim. Change* **66** 9–21

Shi W Q, Chen Q W, Yi Q T, Yu J H, Ji Y Y, Hu L M and Chen Y C 2017 Carbon emission from cascade reservoirs: spatial

heterogeneity and mechanisms *Environ. Sci. Technol.* **51** 12175–81

Smith K R, Desai M A, Rogers J V and Houghton R A 2013 Joint CO_2 and CH_4 accountability for global warming *Proc. Natl Acad. Sci. USA* **110** E2865–74

Sobek S, Tranvik L J and Cole J J 2005 Temperature independence of carbon dioxide supersaturation in global lakes *Glob. Biogeochem. Cycles* **19** GB2003

St. Louis V L, Kelly C A, Duchemin É, Rudd J W M and Rosenberg D M 2000 Reservoir surfaces as sources of greenhouse gases to the atmosphere: a global estimate *BioScience* **50** 766–75

Teodoru C R, Del Giorgio P A, Prairie Y T and Camire M 2009 Patterns in pCO_2 in boreal streams and rivers of northern Quebec, Canada *Glob. Biogeochem. Cycles* **23** GB2012

Tranvik L J, Downing J A, Cotner J B, Loiselle S A, Striegl R G, Ballatore T J, Dillon P, Finlay K, Fortino K and Knoll L B 2009 Lakes and reservoirs as regulators of carbon cycling and climate *Limnol. Oceanogr.* **54** 2298–314

Tremblay A, Varfalvy L, Roehm C and Garneau M 2005 *Greenhouse Gas Emissions Fluxes and Processes* (Berlin: Springer)

Van Breugel Y, Schouten S, Paetzel M, Nordeide R and Sinninghe Damsté J S 2005 The impact of recycling of organic carbon on the stable carbon isotopic composition of dissolved inorganic carbon in a stratified marine system (Kyllaren fjord, Norway) *Org. Geochem.* **36** 1163–73

Wang F S, Cao M, Wang B L, Fu J A, Luo W Y and Ma J 2015 Seasonal variation of CO_2 diffusion flux from a large subtropical reservoir in East China *Atmos. Environ.* **103** 129–37

Wang F S, Lang Y C, Liu C Q, Qin Y, Yu N X and Wang B L 2019a Flux of organic carbon burial and carbon emission from a large reservoir: implications for the cleanliness assessment of hydropower *Sci. Bull.* **64** 603–11

Wang W F, Li S L, Zhong J, Li C, Yi Y B, Chen S N and Ren Y M 2019b Understanding transport and transformation of dissolved inorganic carbon (DIC) in the reservoir system using $\delta^{13}C_{DIC}$ and water chemistry *J. Hydrol.* **574** 193–201

Wang W F, Li S L, Zhong J, Maberly S C, Li C, Wang F S, Xiao H Y and Liu C Q 2020a Climatic and anthropogenic regulation of carbon transport and transformation in a karst river-reservoir system *Sci. Total Environ.* **707** 135628

Wang W F, Yi Y B, Zhong J, Kumar A and Li S L 2020b Carbon biogeochemical processes in a subtropical karst river–reservoir system *J. Hydrol.* **591** 125590

Wanninkhof R 1992 Relationship between wind speed and gas exchange over the ocean *J. Geophys. Res.* **97** 7373–82

Wen Z D, Song K S, Shang Y X, Fang C, Li L, Lv L L, Lv X G and Chen L J 2017 Carbon dioxide emissions from lakes and reservoirs of China: a regional estimate based on the calculated pCO_2 *Atmos. Environ.* **170** 71–81

Xiao J, Wang B L, Qiu X L, Yang M L and Liu C Q 2021 Interaction between carbon cycling and phytoplankton community succession in hydropower reservoirs: evidence from stable carbon isotope analysis *Sci. Total Environ.* **774** 145141

Yang M D, Li X D, Huang J, Ding S Y, Cui G Y, Liu C Q, Li Q K, Lv H and Yi Y B 2020 Damming effects on river sulfur cycle in karst area: a case study of the Wujiang cascade reservoirs *Agric. Ecosyst. Environ.* **294** 106857

Yi Y B, Zhong J, Bao H Y, Mostofa K M G, Xu S, Xiao H Y and Li S L 2021 The impacts of reservoirs on the sources and transport of riverine organic carbon in the karst area: a multi-tracer study *Water Res.* **194** 116933

Zhong J, Li S L, Ibarra D E, Ding H and Liu C Q 2020 Solute production and transport processes in Chinese monsoonal rivers: implications for global climate change *Glob. Biogeochem. Cycles* **34** e2020GB006541